Engineering Chemistry
ISSN: 2813-6535, Vol. 9, pp 85-92
doi:10.4028/p-Z9rTBB

Submitted: 2024-12-28
Revised: 2025-02-19
Accepted: 2025-02-25
Online: 2025-03-10

Adsorptive Removal of Methylene Blue (MB) from Wastewater: A Comparative Modeling Study Utilizing RSM, ANN, and ANFIS Model

Ephraim Igberase[1,a*] and Innocentia Mkhize[2, b]

[1,2]Durban University of Technology, Department of Chemical Engineering, Steve Biko Campus, Durban, South Africa

[a*]ephraimi@dut.ac.za, [b]innocentiaM2@dut.ac.za

Keywords: Response surface; Adsorption; Removal efficiency; Neural network; Chitosan

Abstract. The exceptional properties of chitosan and its effective technique of adsorbing contaminants even to near-zero concentrations are the primary reasons for special attention. The adsorption studies analyzed various elements, such as pH, concentration, reaction time, and adsorbent dose. The study used these factors as input data, with the output data concentrating on MB removal efficiency. For prediction and optimization, MB adsorption used response surface methodology/central composite design (RSM-CCD), artificial neural network (ANN), and adaptive neuron-fuzzy inference system (ANFIS) models. In developing the ANN and ANFIS models, 70% of the data was allocated for training, 15% for validation, and 15% for testing. Based on the RSM-CCD findings, the optimum value for the considered parameters was obtained at pH 7, contact time of 55 min, 6.0 grams of adsorbent, and 125 mg/L adsorbate concentration. However, an ideally trained neural network is described using training, testing, and validation phases, and the R^2 values at these phases were found to be 0.99987, 1, and 1, respectively. The statistical results based on comparative modeling indicated that the ANFIS approach outperformed the RSM and ANN model approaches.

Introduction

The release of dyes into water bodies can have adverse effects on natural creatures and ecosystems. Also, the rapid growth of industrial practices such as leather, food, and paper industries are the primary sources of dyes [1–5]. These dyes, such as cationic dye, are non-biodegradable substances that have a negative impact on humans, such as cancer, Acrimony, skin irritation, allergies, heart attack, and mutations [6]. Because of these hazardous effects, there is an increasing need for resourceful contaminant elimination techniques. Ion exchange, chemical precipitation, adsorption, electrolysis, Filtration, and sedimentation are some methods that have been applied to maximize the number of pollutants in wastewater. Adsorption is among the most effective techniques because it is inexpensive and environmentally friendly process for removing dyes [7]. Various materials such as chitosan, zeolites, and many more are used as active adsorbents. Chitosan is considered an ideal adsorbent for dye removal since it is environmentally friendly. However, chitosan is said to be soluble in acid solution, limiting its use in adsorption studies; therefore, cross-linking using cross-linkers such as glutaraldehyde is required to make the substance insoluble at low pH. Several studies, including [8,9], have suggested that cross-linking lowers chitosan's adsorption ability. This observation may be because some amine groups are used up during cross-linking reactions. As a result, grafting some functionality onto the cross-linked material becomes vital. Grafting chitosan allows for the formation of functional derivatives by covalently attaching a molecule to the backbone of chitosan. This technique is frequently used to improve the binding qualities of chitosan.

This research investigated how RSM, ANN, and ANFIS models explain the relationship and essential dynamics of the process variables. A new contribution to adsorption studies is a comparative assessment of these techniques for forecasting MB adsorption using a chitosan derivative in synthetic wastewater. This study offers a clear road map for choosing suitable models depending on the adsorption system complexity, availability of data, and the intended agreement between interpretability and accuracy by highlighting the result of the R^2 discrepancy. This knowledge closes the gap between creating theoretical models and real-world implementation in environmental and industrial adsorption research. ANFIS balances accuracy and interpretability. RSM is best for simplicity, while ANN is accurate for pure prediction. The decision is based on the problem's complexity and the requirement for interpretability. This study also provides the groundwork for using hybrid intelligence systems in further adsorption research by proving that ANFIS is a better option than conventional RSM and ANN. This could result from improved predicted accuracy in practical applications, lower experimental costs, and more effective system designs. Although [10] and [11] showed that ANN is more accurate than RSM in predicting adsorption efficiency, they also pointed out that overfitting was a problem when training limited datasets. On the other hand, this study applied a regularized ANN model with a larger dataset, which led to a considerable decrease in overfitting and improved prediction performance. This work also found that ANFIS is the most reliable model by surpassing both RSM and ANN in capturing nonlinear dynamics, a result that has never been documented in adsorption studies of this magnitude. These developments demonstrate how hybrid machine-learning models can improve the design of adsorption systems. The study's results could facilitate the development and refinement of adequate water treatment systems and the choice of the optimal modeling method for adsorption processes and also contribute significantly to the emerging field of predictive modeling in adsorption studies by explaining the comparative advantages of RSM, ANN, and ANFIS.

Material and Methods

Analytical-grade chemicals from Sigma-Aldrich, South Africa, were used in this study. These chemicals include Sodium hydroxide, ethanol, hydrochloric acid, acetic acid, glutaraldehyde, MB, and aniline, with a purity level of 99%. pH meter was used to maintain the pH level of the solution and was obtained from China. To produce the stock solution for MB, 1g of MB was dissolved in 1L of distilled water to achieve the 1000 mg/L stock solution. The stock solution was again diluted to different initial concentrations of Methyl-Blue. Chitosan (MW=2.0×10^5g/mol) was obtained from Tokyo, Japan. Chitosan solution was prepared by diffusing 30g of chitosan powder in 1L of 5.0% (V/V) acetic acid. The prepared solution was pipetted into 1M sodium hydroxide solution to create chitosan gel beads. The beads were transferred into a beaker containing 2.5% glutaraldehyde solution and agitated for 2 hours for a cross-linking reaction. The cross-linked beads were grafted with aniline using a microwave oven. The functional groups that are available for binding were shown using FTIR. The infrared spectra of the beads were done with Shimadzu FTIR model 8300 Kyoto, Japan. The spectra were estimated between 500-4000cm^{-1}. In the adsorption study, a BIS incubator shaker from China was used to stir the beakers at an observed rotating speed of 250 RPM.

Results and Discussion

FTIR Analysis

Infrared spectroscopy was utilized to demonstrate comparable differences between chitosan (XB), cross-linked chitosan (XXB), and grafted cross-linked chitosan (GXXB) in Figure 1. The broadband shows amine and hydroxyl groups at wavelengths 3381 cm^{-1}, 3389 cm^{-1}, and 3396 cm^{-1} XB, XXB, and GXXB, respectively. The shift in the band might be due to exchangeable protons during the modification process [12]. XB and XXB demonstrated the presence of oxygenated functional groups from alcohols and aliphatic ethers at wavelengths of 1000 cm^{-1}. It suggests that specific properties of the XB material were maintained even after modification. However, the wavelength changed to 1020 cm^{-1} when the cross-linked beads were grated, which also provided evidence of a successful modification process.

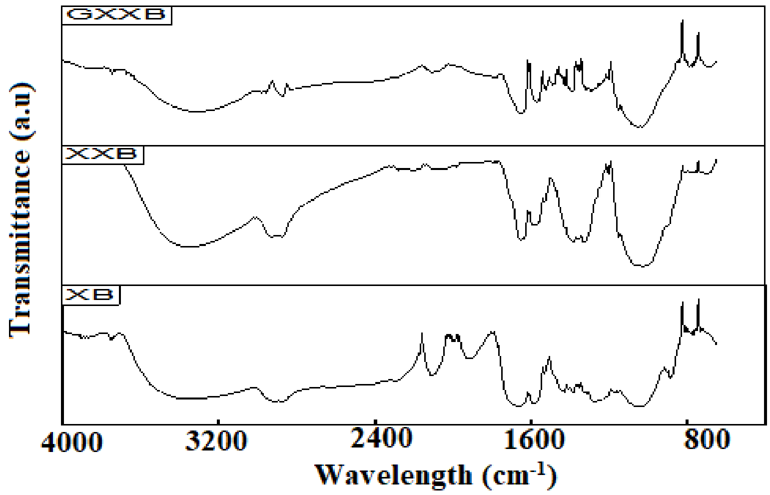

Fig. 1. FTIR of pattern XB, XXB, and GXXB respectively.

Response Surface Methodology Analysis

Table 1 presents the experimental design/matrix and the related response for binding MB onto GXXB using RSM/CCD. This table illustrates how various parameters impact the outcome. Using analysis of variance (ANOVA), the effect of solution pH, MB concentration, GXXB dose, and contact time on MB removal efficiency was determined. Eq. 1 displays the quadratic polynomial equation. A correlation coefficient (R^2) of 0.999 was obtained for both experimental and predicted values.

$$\gamma_{Pb} = +92.24 - 5.50A + 1.00B - 8.17C - 0.50D - 5.77A^2 - 2.27B^2 - 3.43C^2 - 16.77D^2 - 10.50AB - 0.75AC - 6.25AD + 1.00BC - 5.00BD + 3.25CD \quad (1)$$

Table 1. Design matrix showing the input variables and response.

STD	Factor 1 A: pH	Factor 2 B: Adsorbent dose (g)	Factor 3 C: Initial concentration (mg/L)	Factor 4 D: Reaction time (Min)	Response: Removal efficiency of MB (%)
1	10.00	2.00	200.00	100.00	49.63
2	10.00	2.00	50.00	100.00	72.07
3	10.00	10.00	200.00	10.00	59.63
4	4.00	10.00	50.00	100.00	85.07
5	10.00	10.00	50.00	10.00	73.07
6	4.00	2.00	200.00	10.00	35.63
7	4.00	10.00	200.00	100.00	78.63
8	4.00	2.00	125.00	10.00	59.07
9	4.00	6.00	125.00	55.00	91.61
10	10.00	6.00	125.00	55.00	80.61
11	7.00	6.00	125.00	10.00	88.61
12	7.00	6.00	50.00	100.00	90.79
13	7.00	6.00	50.00	55.00	96.41
14	7.00	6.00	125.00	55.00	80.48
15	7.00	2.00	125.00	55.00	75.61
16	7.00	10.00	125.00	55.00	74.61
17	7.00	6.00	125.00	55.00	93.47
18	7.00	6.00	125.00	55.00	92.47
19	7.00	6.00	125.00	55.00	92.47
20	7.00	6.00	125.00	55.00	92.47
21	7.00	6.00	125.00	55.00	92.47

Three Dimensional (3D) RSM plots

The results obtained from the 3D RSM-CCD analysis are shown in Figure 2 (a-d). The graph demonstrates the correlation between two factors and their effect on the removal efficiency of MB when other parameters are kept constant. Figure 2 (a-c) shows that the optimum removal efficiency of MB on GXXB occurred at pH 7, illustrating the importance of pH on the binding of pollutants. The results of [5] indicate that pH is crucial to adsorption processes because it can significantly impact the ionization of chemically reactive sites on the adsorbent's surface. Figure 2 (a and d) illustrates that the adsorbent dosage is an essential factor influencing the binding of pollutants. However, raising the mass of GXXB employed in adsorption studies can decrease the charge of the outer layer of cells, resulting in the blockage of binding sites needed for MB adsorption. Previous studies have documented this behavior [9,10]. The influence of reaction time on pollutant binding is depicted in Figure 2 (a and d). The reaction time was varied from 10 to 100 min, and it was shown that a contact time of 55 minutes was sufficient for maximal MB removal. This is due to the availability of well-aligned binding sites for the adsorption of MB. Figure 2 (b and d) shows how the initial concentration affects the removal efficiency of MB. However, at lower initial concentrations of MB, the process of adsorption is not affected by the starting concentration. This is due to the small quantity of GXXB compared to the large proportion of pollutant cations. A higher initial concentration of MB increases the amount of MB available, resulting in improved percentage removal for a fixed mass of GXXB.

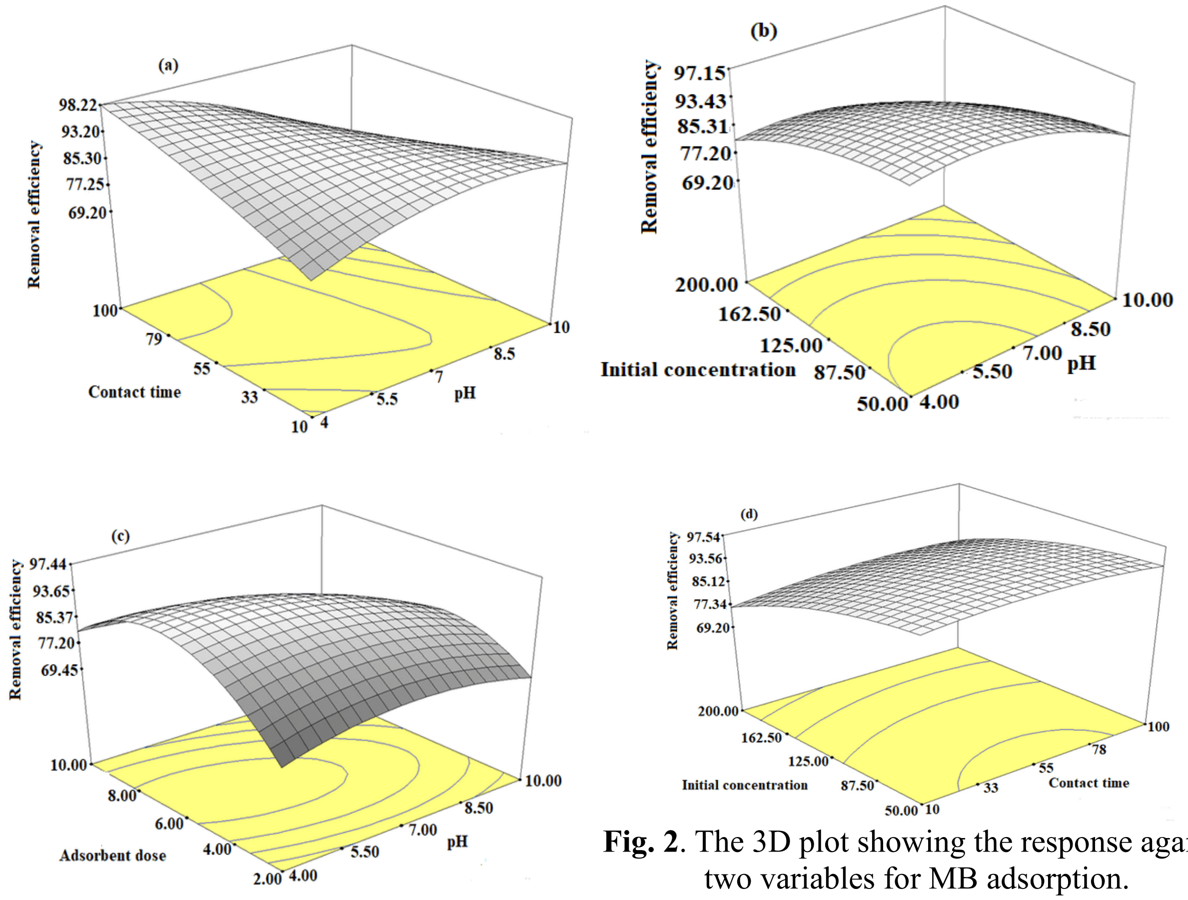

Fig. 2. The 3D plot showing the response against two variables for MB adsorption.

ANN result

This study used the ANN approach with the ANN Toolbox V4.0 in MATLAB 2019. The Levenberg-Marquardt (LM) coding process conditions changed as the network parameters were adjusted. Figure 3 shows the ANN architecture, while Figure 4 shows how the network correlated with the training, testing, and validation data. The correlation coefficients were respectively found to be 0.99987, 1, 1, and 0.91416 for training, testing, validation, and overall data. The predicted results from the model correlate with the experimental data. The ANN model has great prediction ability, as shown by the overall correlation coefficient, and is suited for accurately predicting data.

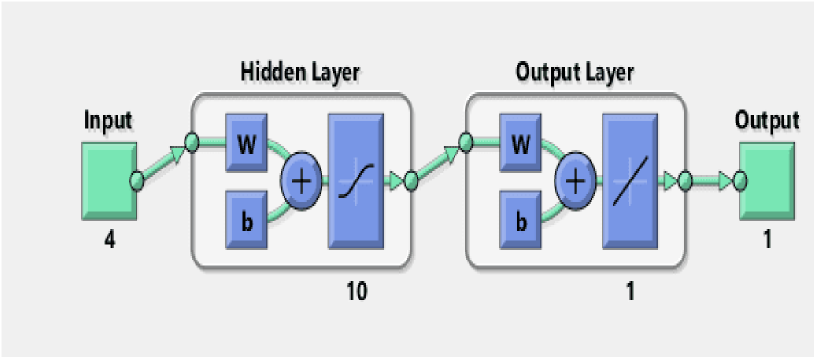

Fig. 3. The ANN architecture and LM algorithm in predicting removal efficiency of MB by GXXB.

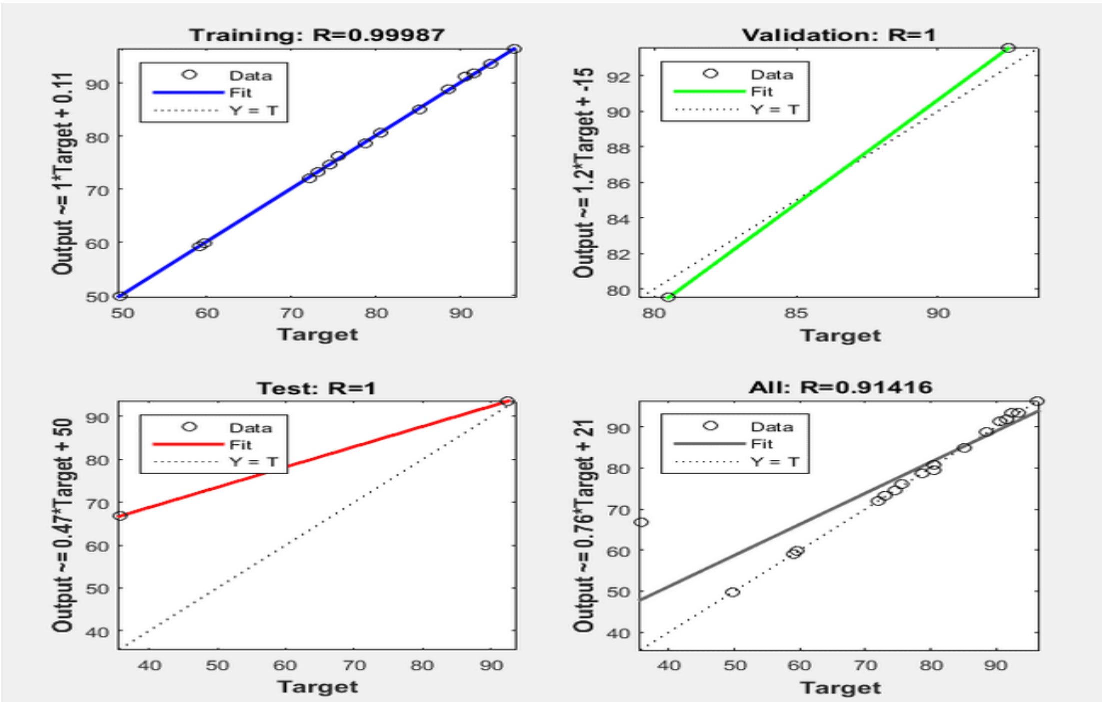

Fig. 4. The network response regression analysis results between the ANN output and the corresponding target.

ANFIS modelling

A fuzzy inference system approach was used to create the four-layered neural network [13]. To generate the fuzzy network, each parameter in the input layer was given three membership functions (MFs), as seen in Figure 5. The high correlation value of 0.999 obtained from the ANFIS model suggests that the fuzzy inference system network can accurately forecast the removal efficiency of MB from the solution using GXXB. The primary benefit of ANFIS is that it lowers errors by adding self-learning capabilities to fuzzy controllers [13]. The fuzzy network demonstrated an error size of 0.005 after seven training epochs, indicating that it is suitable for modeling the removal of MB. Furthermore, the low MSE value showed that there was no over-fitting during the training process and that the ANFIS model could accurately determine the binding of MB by GXXB. One of the strengths of ANFIS in adsorption studies is its skill in dealing with numerical variable input. As a result, it serves as a valuable tool for modeling systems facing data uncertainties or challenges in measuring some input variables. Figure 5 describes a hierarchical structure of fuzzy inference systems.

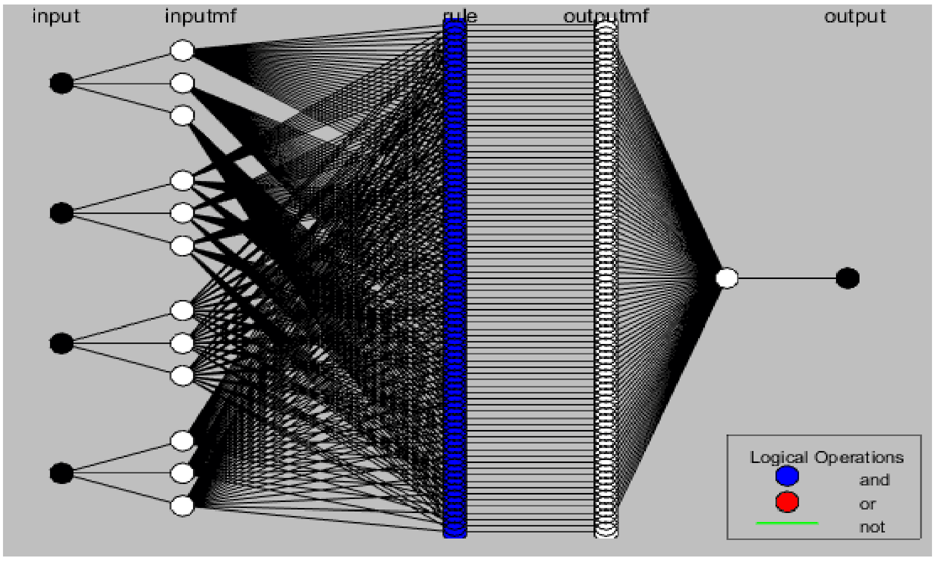

Fig. 5. ANFIS architecture describing a four-layer input neural network using a fuzzy inference system approach.

Statistical prediction of the models

Table 2 displays the parameters and data utilized in the training procedure based on the ANFIS and ANN models. The analysis of predicted and actual removal rates illustrates that these models can effectively predict data from the experiment. To correlate the three models, statistical analysis was utilized to investigate the significance and distribution of errors in the expected removal efficiency. The outcomes of the statistical analysis are displayed in Table 3. However, the table compares the error functions obtained by the ANN, ANFIS, and RSM models. ANFIS outperformed ANN and RSM by achieving a lower error function. Consequently, the R^2 values for the three models exhibit a high degree of similarity, describing a good correlation between the anticipated and actual data. Consequently, the quality and unpredictability of wastewater data present several obstacles to the practical application of RSM, ANN, and ANFIS in wastewater treatment, which may compromise the accuracy and dependability of the models. Complex nonlinear interactions are complicated for RSM to capture. While ANN works well for these systems, it needs large, high-quality datasets and can overfit or generalize poorly to other plants. Even though ANFIS is more resilient to noise and uncertainty, configuring it for large-scale systems can be time-consuming and computationally demanding. The model's applicability is further limited by variations in pollutant kinds, treatment technologies, and operating conditions, which further restrict scalability and adaptability. Furthermore, real-time adaptation and control require computational resources that might not be easily accessible, and plant operators may find it challenging to understand and implement ANN and ANFIS without specialized knowledge. Integrating these models into realistic wastewater treatment processes is made more difficult by operational and financial limitations, such as tight budgets and a lack of technical expertise.

However, regarding computational demand and data requirements, RSM is computationally efficient, but it requires well-designed experimental datasets and has difficulty dealing with nonlinear systems. ANN can model complicated relationships but requires vast, high-quality datasets and is computationally expensive, particularly for large-scale processes. Furthermore, significant resources are needed for retraining and fine-tuning. ANFIS compromises interpretability and accuracy, but as inputs and fuzzy rules increase, it becomes resource-intensive and depends on structured datasets for efficient rule building. These restrictions highlight the importance of guaranteeing sufficient processing power and data quality for real-world applications.

Table 2. Back-propagation data employed in the ANFIS and ANN models

ANFIS model		ANN model	
Characteristic	Value	Characteristic	Results
Fuzzy rules	34	Epochs number	30
Checking data	4	Learning rule	Levenberg
Testing data	4	Output nodes	1
Training data	18	Input nodes	4
Number of parameters	26	Number of neurons	10
Linear parameters	208	Error	0
Non-linear parameters	314	Mu	10e-5
Number of nodes	320		

Table 3. ANN, ANFIS, and RSM statistical metrics for non-linear error function fit.

Statistical function	ANN	ANFIS	RSM
MPSD	0.0061	0.0082	0.0693
χ^2	0.0019	0.0026	0.0432
RMSE	0.0032	0.0043	0.0966
MSE	0.0030	0.0021	0.0665
SSE	0.0022	0.0044	0.0322
ARE	0.0058	0.0065	0.0984

Conclusion

This study presents an efficient prediction model for MB adsorption utilizing GXXB as an adsorbent. The L–M algorithm (4-10–1) with the ANN approach produced a low MSE. ANFIS, ANN, and RSM were shown to be equivalent and dependable in MB uptake prediction. Five statistical functions showed that the ANFIS model is the most reliable and produces the best outcome, followed by the ANN and RSM models. A three-layer back-propagation neural network was developed to describe MB binding in a synthetic mixture. The outcomes of these models demonstrated that they could adequately predict and reproduce the behavior of the process. The adsorption of MB was represented by equations that were developed using experimental data sets. This study can be scaled up by focusing on the bulk production of cost-effective, long-lasting, and reusable GXXB. Also, pilot-scale testing and process optimization with RSM, ANN, and ANFIS can improve dye removal efficiency in real-world conditions. Continuous flow systems should be adopted, and dynamic control should be automated with predictive models. Finally, ensure economic viability, environmental sustainability, and regulatory compliance for wastewater discharge.

Acknowledgments

The author wishes to thank the Durban University of Technology's Department of Chemical Engineering for providing continuous working facilities.

References

[1] A. Mokhtar, S. Abdelkrim, A. Djelad, A. Sardi, B. Boukoussa, M. Sassi, A. Bengueddach, Adsorption behavior of cationic and anionic dyes on magadiite-chitosan composite beads, Carbohydr Polym 229 (2020). https://doi.org/10.1016/j.carbpol.2019.115399.

[2] J. Geng, L. Lin, F. Gu, J. Chang, Adsorption of Cr(VI) and dyes by plant leaves: Effect of extraction by ethanol, relationship with element contents and adsorption mechanism, Ind Crops Prod 177 (2022). https://doi.org/10.1016/J.INDCROP.2022.114522.

[3] A. Mokhtar, B. Boukoussa, A. Baba Ahmed, S. Abdelkrim, A. Djelad, M. Hachemaoui, F. Zaoui, A. Bengueddach, M. Sassi, Alginate@Layered Silicate Composite Beads: Dye Elimination, Box–Behnken Design Optimization and Antibacterial Property, J Inorg Organomet Polym Mater 32 (2022) 2615–2633. https://doi.org/10.1007/s10904-022-02350-9.

[4] L.D. Pompeu, P.C.L. Muraro, G. Chuy, B.S. Vizzotto, G. Pavoski, D.C.R. Espinosa, L. da Silva Fernandes, W.L. da Silva, Adsorption for rhodamine b dye and biological activity of nano-porous chitosan from shrimp shells, Environ Sci and Pollut Res 29 (2022) 49858–49869. https://doi.org/10.1007/s11356-022-19259-y.

[5] A. Mokhtar, S. Abdelkrim, B. Boukoussa, M. Hachemaoui, A. Djelad, M. Sassi, M. Abboud, Elimination of toxic azo dye using a calcium alginate beads impregnated with NiO/activated carbon: Preparation, characterization and RSM optimization, Int J Biol Macromol 233 (2023). https://doi.org/10.1016/j.ijbiomac.2023.123582.

[6] N. Ali, A. Hameed, S. Ahmed, Physicochemical characterization and Bioremediation perspective of textile effluent, dyes and metals by indigenous Bacteria, J Hazard Mater 164 (2009) 322–328. https://doi.org/10.1016/j.jhazmat.2008.08.006.

[7] D.N. Poshina, S. V. Raik, A.N. Poshin, Y.A. Skorik, Accessibility of chitin and chitosan in enzymatic hydrolysis: A review, Polym Degrad Stab 156 (2018) 269–278. https://doi.org/10.1016/j.polymdegradstab.2018.09.005.

[8] P.O. Osifo, A. Webster, H. van der Merwe, H.W.J.P. Neomagus, M.A. van der Gun, D.M. Grant, The influence of the degree of cross-linking on the adsorption properties of chitosan beads, Bioresour Technol 99 (2008) 7377–7382. https://doi.org/10.1016/j.biortech.2008.01.053.

[9] G. Rojas, J. Silva, J.A. Flores, A. Rodriguez, M. Ly, H. Maldonado, Adsorption of chromium onto cross-linked chitosan, Sep Purif Technol 44 (2005) 31–36. https://doi.org/10.1016/j.seppur.2004.11.013.

[10] J. Kabuba, M. Banza, Ion-exchange process for the removal of Ni (II) and Co (II) from wastewater using modified clinoptilolite: Modeling by response surface methodology and artificial neural network, Results Eng 8 (2020). https://doi.org/10.1016/j.rineng.2020.100189.

[11] M. Banza, H. Rutto, T. Seodigeng, Application of Artificial Neural Network and Shrinking Core Model for Copper (Ii) and Lead (Ii) Leaching from Contaminated Soil Using Ethylenediaminetetraacetic Acid, Soil Sediment Contam (2023). https://doi.org/10.1080/15320383.2023.2178384.

[12] E. Igberase, P. Osifo, A. Ofomaja, Chromium (VI) ion adsorption by grafted cross-linked chitosan beads in aqueous solution–a mathematical and statistical modeling study, Environ Technol (United Kingdom) 38 (2017) 3156–3166. https://doi.org/10.1080/09593330.2017.1290152.

[13] C.E. Onu, J.T. Nwabanne, P.E. Ohale, C.O. Asadu, Comparative analysis of RSM, ANN and ANFIS and the mechanistic modeling in eriochrome black-T dye adsorption using modified clay, S Afr J Chem Eng 36 (2021) 24–42. https://doi.org/10.1016/j.sajce.2020.12.003.